Phyton-
International Journal of
Experimental Botany

Tech Science Press

Doi:10.32604/phyton.2025.069166

ARTICLE

RAPD Marker Associations and Antioxidant Enzyme Responses of *Houttuynia cordata* Germplasms under Lead Stress

Yi Yan[1,2,#], Min He[1,2,#], Feifeng Mao[3], Xinyu Zhang[4], Liyu Wang[5] and Jingwei Li[1,2,*]

[1]Vegetable Industry Research Institute, Guizhou University, Guiyang, 550000, China
[2]Agricultural College, Guizhou University, Guiyang, 550000, China
[3]Department of Agriculture and Rural Affairs, Guizhou Province, Guiyang, 550000, China
[4]Fruit and Vegetable Technical Guidance Station, Wusheng County, Wusheng, 638499, China
[5]Agricultural and Rural Bureau, Qiannan Buyei and Miao Autonomous Prefecture, Duyun, 558000, China

*Corresponding Author: Jingwei Li. Email: ljw198@yeah.net

[#]These authors contributed equally to this work

Received: 16 June 2025; Accepted: 04 September 2025; Published: 29 October 2025

ABSTRACT: *Houttuynia cordata*, a characteristic edible and medicinal plant in southwestern China, is prone to absorbing lead (Pb^{2+}). Excessive consumption may lead to Pb^{2+} accumulation in the human body, which has been linked to serious health risks such as neurotoxicity, kidney damage, anemia, and developmental disorders, particularly in children. Therefore, the development of molecular markers associated with Pb^{2+} uptake and the investigation of the plant's physiological responses to Pb^{2+} pollution are of great significance. In this study, 72 *H. cordata* germplasms were evaluated for Pb^{2+} accumulation after exogenous Pb^{2+} treatment. A significant variation in Pb^{2+} content was observed among the germplasms, indicating rich genetic diversity. Using RAPD markers, seven loci were identified to be significantly associated with Pb^{2+} uptake, with locus 43 (R^2 = 6.72%) and locus 53 (R^2 = 5.39%) showing the strongest correlations. Marker validation was performed using five low- and five high-accumulating accessions. Two representative germplasms were further subjected to 0, 500 and 1000 mg/kg Pb^{2+} treatments for 40 days. Pb^{2+} content, membrane lipid peroxidation, and redox enzyme activities (SOD, POD and CAT) were measured across different organs. Organs with greater soil contact (roots) exhibited higher Pb^{2+} accumulation and oxidative damage. POD and CAT activities were markedly induced by Pb^{2+} stress, while SOD response was limited. This study provides a theoretical foundation for breeding low Pb^{2+}-accumulating *H. cordata* varieties through marker-assisted selection (MAS) and supports their safe use and application in phytoremediation.

KEYWORDS: *Houttuynia cordata*; germplasm resources; lead (Pb^{2+}); RAPD; lipid oxidation

1 Introduction

Houttuynia cordata, a highly popular vegetable in Southwest China, belongs to the Saururaceae family. This versatile plant serves dual purposes as both a vegetable crop and a medicinal herb. Studies have demonstrated its potent inhibitory effects on viral infections [1,2]. Furthermore, *H. cordata* boasts antibacterial, antioxidant, and antitumor properties [3–5], making it a valuable asset in alleviating inflammation. China is endowed with abundant germplasm resources of *H. cordata*, and its utilization spans a lengthy historical period [4]. Beyond its medicinal and edible worth, this plant finds applications in the production of fermented beverages, health supplements, and cosmetics, further underscoring its multifaceted utility [6].

Pb^{2+} contamination poses a worldwide challenge [7], manifesting in diverse forms in the natural environment. This contamination can lead to varying degrees of environmental pollution, impacting soil, plants, water, air, and other vital components closely intertwined with human life [8–11]. Exposure to Pb^{2+}-contaminated environments may result in different levels of Pb^{2+} poisoning towards humans [12]. Excessive intake of lead can easily lead to the accumulation of lead ions (Pb^{2+}) in the human body. Its harm not only involves serious health risks such as neurotoxicity, kidney damage, anemia and developmental disorders, but also has a particularly significant impact on children. Furthermore, crops cultivated in Pb^{2+}-contaminated soil pose significant safety risks to agricultural produce [13], thereby elevating the likelihood of Pb^{2+} poisoning in human tissues and organs [14–17].

H. cordata has a propensity for absorbing heavy metals. In China, numerous studies have demonstrated its strong ability to absorb Pb^{2+}. Wang et al. [18] employed Inductively coupled plasma mass spectrometry (ICP-MS) to confirm the robust absorption capacity of *H. cordata* for lead (Pb^{2+}). Li [19] found that *H. cordata* has a certain absorption capacity for Cd^{2+}, As^{3+}/As^{5+}, and Pb^{2+}, with the strongest absorption for Pb^{2+}, aligning with the results of the study of Zhao et al. [20]. The rhizomes, serving as the primary edible portion, exhibit a remarkable tolerance for Pb^{2+} concentrations as high as 1000 mg/kg [21]. In light of *H. cordata*'s strong absorption capacity for Pb^{2+}, concerns arise regarding the safety of its consumption and use.

Molecular markers refer to DNA sequences located at specific positions within the genome, which, due to their polymorphic characteristics, can reveal genetic variations among different individuals. Association analysis between heavy metal absorption and molecular markers facilitates molecular breeding for plant resistance to heavy metal stress. Nie et al. [22] conducted measurements of Cr^{6+} content in *Liriodendron chinense* treated with 200 mg/L Cr^{6+} and subsequently performed a general linear model Generalized linear model (GLM) analysis with Expressed sequence tags-simple sequence repeat (EST-SSR) markers. At a significance level of $p < 0.05$, 46 loci were found to be associated. Huang et al. [23] employed QTL mapping and identified molecular marker loci associated with the absorption of Cd^{2+}, Zn^{2+}, or selenium (Se^{4+}/Se^{6+}) on chromosomes 5, 7 and 11, respectively, with molecular marker loci related to Pb^{2+} absorption present on all three of these chromosomes. Williams et al. [24] were the first to discover and report the Randomly amplified polymorphic DNA (RAPD) technique for molecular markers. The principle of this technique involves using random primers of 8–10 base pairs in length to amplify DNA fragments at non-specific loci through polymerase chain reaction (PCR) reactions [25]. RAPD offers advantages such as ease of operation, low cost, minimal requirements for DNA quality, and no prior knowledge of DNA sequence information being necessary [26].

Pb^{2+} contamination induces profound physiological effects on plants. A comparative analysis of *Zea mays* planted in soil with or without high Pb^{2+} contamination revealed that plants subjected to Pb^{2+} stress exhibited significantly elevated levels of malondialdehyde (MDA), and stimulated activities of redox enzymes, for instance, activities of superoxide dismutase (SOD), peroxidase (POD), and catalase (CAT), compared to their non-stressed counterparts [27]. In contrast, research on *Picea asperata* seedlings under Pb^{2+} stress observed a notable decline in their antioxidant enzyme activities [28]. When *Alnus cremastogyne* trees were cultivated in soil with varying Pb^{2+} concentrations (ranging from 0 to 400 mg/kg), the findings indicated that as Pb^{2+} concentrations increased, the activities of antioxidant enzymes and the content of osmolytes initially rose but eventually declined [29]. In living organisms, redox enzymes work in tandem to scavenge oxygen radicals and peroxides, effectively inhibiting membrane lipid peroxidation and protecting cellular membranes from damage or destruction. Under adverse environmental conditions, such as heavy metal contamination, the concentration of reactive oxygen species (ROS) in plants surges considerably. These excessive ROS can directly or indirectly initiate peroxidation of membrane lipids, a process that, akin to a

chain reaction, irreversibly generates additional radicals, thereby exacerbating damage to cellular structure and function.

In this study, we assessed the Pb^{2+} absorption capacity of 72 *H. cordata* samples under high Pb^{2+} contamination conditions. DNA was extracted from each germplasm, and RAPD molecular marker analysis was conducted. By analyzing the patterns of PCR products, combined with the Pb^{2+} absorption characteristics of the germplasms, correlation analysis was performed to identify potential molecular markers or loci indicative of Pb^{2+} absorption capacity in *H. cordata*. A pair of *H. cordata* materials with extremely high and low Pb^{2+} absorption capacities were selected and planted in substrates with varying Pb^{2+} concentrations. By examining Pb^{2+} content, MDA content, and activities of SOD, POD, and CAT enzymes in different organs of this pair, the spatial distribution pattern of Pb^{2+} within *H. cordata* and the physiological impact mode of Pb^{2+} on the plant were analyzed. The research data provide a foundational dataset for molecular-assisted breeding of *H. cordata* with low Pb^{2+} absorption capacity.

2 Materials and Methods

2.1 Plant Materials

In this study, 72 accessions of *H. cordata* germplasms served as the plant materials. In order to investigate their ability to absorb Pb^{2+}, The rhizomes of *H. cordata* were cultivated in a Pb^{2+}-contaminated substrate composed of equal parts (1:1:1) of peat, vermiculite, and perlite. A 500 mg/kg Pb^{2+} solution was added to 3 kg of dry substrate, mixed thoroughly, and then filled into pots. Following 40 d of repeated watering and air-drying cycles, a naturally passivated Pb^{2+}-contaminated substrate was obtained. The reagent used for preparing the Pb^{2+}-contaminated substrate was analytical-grade lead nitrate solution ($Pb(NO_3)_2$, TMRM, Beijing, China). The rhizomes of *H. cordata*, each consisting of three nodes, were planted in the Pb^{2+}-contaminated and uncontaminated substrate. For each treatment, 30 g of stem segments were planted at a depth of 5 cm. The plants were uniformly managed with water and fertilizer according to standard cultivation practices for a period of 180 days, with no additional fertilizers, growth regulators, or other agents applied throughout this duration.

2.2 Determination of Pb^{2+} Content in the Rhizomes of H. cordata

The content of Pb^{2+} in *H. cordata* was determined by ICP-MS according to Paul et al. [30] with some mofidication. The Pb^{2+} content in *H. cordata* was determined using inductively coupled plasma mass spectrometry (ICP-MS). Fresh samples were first rinsed with tap water and ultrapure water, oven-dried at 60°C, and ground into a fine powder. Powder of 0.3 g was weighed into microwave digestion vessels and digested with 5 mL of concentrated nitric acid (HNO_3, 65%) and 2 mL of hydrogen peroxide (H_2O_2, 30%) using a microwave digestion system. The digested solution was evaporated to near dryness at 140°C, diluted to 50 mL with 2% HNO_3, and filtered through a 0.22 μm membrane. Pb^{2+} concentrations were measured using a Thermo Fisher iCAP Qc ICP-MS. Standard solutions (0–10 μg/L) were prepared using 2% HNO_3, with a 10 μg/L internal standard solution added for calibration. The absorptivity of Pb^{2+} is determined as the difference value of Pb^{2+} content of 500 mg/kg Pb^{2+} treated samples minus Pb^{2+} content of 0 mg/kg Pb^{2+} treated samples. The external standard method was used to calculate Pb^{2+} content based on the following equation:

$$pb^{2+}(\mu g/g) = \frac{\text{Final concentration ICP} - \text{MS}\ (\mu g/mL) \times 50\ mL}{\text{Sample weight}\ (g)}$$

2.3 RAPD Reaction

DNA extraction was conducted according to Zhu et al. [31]. The 34 RAPD primer sequences used in this experiment were sourced from Wu et al. [32], and the synthesis of the primers was commissioned to Sangon Biotech (Shanghai, China) Co., Ltd. A total of 8 primers producing clear polymorphic bands were screened out for experimental and statistical analysis (Table 1). The PCR mix system was 20 μL, containing 2 μL of template DNA, 1 μL of primer, 10 μL of 2× Taq enzyme, and 7 μL of ddH_2O. The PCR program was as follows: initial denaturation at 94°C for 3 min, followed by 35 cycles of denaturation at 94°C for 1 min, annealing at 53°C for 1 min, and extension at 72°C for 2 min. After the last cycle, the mixture was kept at 72°C for 10 min. The amplified products were separated by electrophoresis on a 1.5% agarose gel. The results were observed and photographed on a ChampChemi610 (Beijing Sai zhi, Beijing, China).

Table 1: RAPD primer sequences and source

Primer names	Sequences (5′–3′)
OPA-10	GTGATCGCAG
OPA-15	TTCCGAACCC
OPA-20	GTTGCGATCC
OPH-05	AGTCGTCCCC
OPH-06	ACGCATCGCA
OPH-07	CTGCATCGTG
OPH-12	ACGCGCATGT
OPH-19	CTGACCAGCC

2.4 Correlation Analysis of RAPD Molecular Markers and Pb^{2+} Content

To assess the relationship between RAPD molecular markers and Pb^{2+} content in *H. cordata*, we conducted an association analysis using a GLM implemented in TASSEL 5.2 software. In this model, the Pb^{2+} content for each accession (log-transformed to approximate normal distribution) was used as the dependent variable, and the presence/absence (1/0) of each RAPD locus was treated as an independent predictor. For each RAPD locus, the model calculated the F-statistic to test the significance of its effect on Pb^{2+} content, along with the corresponding p-value derived from the F-distribution. To assess the robustness of the observed associations, a permutation test (1000 permutations of genotype-phenotype assignments) was performed to calculate empirical permutation p-values (Perm p). Additionally, the phenotypic variation explained by each marker was reported as the coefficient of determination (R^2), representing the proportion of total variance in Pb^{2+} content attributable to each marker. Significance was determined at the nominal level of $p < 0.05$. Although permutation p-values were not significant for individual loci, further validation was conducted using five accessions with the highest and five with the lowest Pb^{2+} content, to confirm the consistency of marker-locus patterns.

2.5 Detection of Pb^{2+} Content in Different Organs of H. cordata

Due to the low reproduction rate of GZZZ (the lowest Pb^{2+} absorbent germplasm) and the insufficient sample amount to be tested, *H. cordata* GZNJ1 and GZSCP were used as experimental materials. GZNJ1 and GZSCP were the Pb^{2+} second-lowest and the highest absorption germplasms, respectively. The rhizomes of two germplasms were planted on Pb^{2+}-contaminated cultivation substrate (Pb^{2+} concentrations of 0, 500 and 1000 mg/kg, respectively). These three levels were chosen to establish a dose response range from moderate to high Pb stress in pots; the 1000 mg/kg level was included to elicit clear phenotypic and physiological

differences among germplasms under controlled conditions. Each rhizome carried 3 internodes, and each treatment cultivated a total of 30 g stem segments. The planting depth of the stem segments was 5 cm, and each experimental treatment was repeated 3 times. After 40 d of treatment, *H. cordata* fibrous roots, rhizomes, stems and leaves were taken and washed with tap water, washed with deionized water 3 times, and then dried with absorbent paper to remove excess water. ICP-MS was used to determine the Pb^{2+} content in each organ.

2.6 Determination of MDA Content of Different Organs of H. cordata

Forty-day-old adventitious roots, rhizomes, stems, and leaves of 0, 500 and 1000 mg/kg Pb^{2+} treated *H. cordata* were collected. The samples were washed with tap water, followed by 3 rinses with deionized water, and then dried with absorbent paper to remove excess water. The samples were then ground into a homogenate. The content of MDA was determined according to the instructions provided by MDA assay kit (TBA method) (A003-1-2, Nanjing Jiancheng, Nanjing, China).

2.7 Determination of Activities of Redox Enzymes in Different Organs of H. cordata

After 0, 500 and 1000 mg/kg Pb^{2+} treatment, 40 d adventitious roots, rhizomes, stems, and leaves of *H. cordata* were collected. The samples were washed as described above and then ground into a homogenate. The activities of SOD, POD, and CAT were determined according to the instructions provided by SOD Activity Assay Kit (BC0175, Solarbio, Beijing, China), POD Activity Assay Kit (BC0090, Solarbio) and CAT Activity Assay Kit (BC0205, Solarbio), respectively.

2.8 Data Analysis

All experiments were repeated at least three times, with each replicate containing no fewer than 30 biological samples. The data are presented as mean ± standard error (SE). Statistical significance ($p < 0.05$) was determined using one-way analysis of variance (ANOVA).

3 Results

3.1 The Pb^{2+} Content in the Rhizomes of H. cordata

Among the 72 accessions of *H. cordata*, one accession had a Pb^{2+} content below 1.00 mg/kg, which was GZZZ (at 0.32 mg/kg). There were 19 accessions with Pb^{2+} content ranging from 1.00 to 2.00 mg/kg. Among these, the accession with the lowest Pb^{2+} content was GZNJ1, at 1.16 mg/kg, followed by GZZZ. The accession with the highest Pb^{2+} content in this range was GZLL9, at 1.99 mg/kg. There were 23 accessions with Pb^{2+} content ranging from 2.00 to 3.00 mg/kg. The lowest in this range was GZGY, with a Pb^{2+} content of 1.97 mg/kg, while the highest was GZLT, with a Pb^{2+} content of 2.98 mg/kg. Fifteen accessions had Pb^{2+} content ranging from 3.00 to 4.00 mg/kg. The lowest in this range was CQWX, with a Pb^{2+} content of 3.08 mg/kg, and the highest was SCMS, with a Pb^{2+} content of 3.98 mg/kg. Six accessions had Pb^{2+} content ranging from 4.00 to 5.00 mg/kg. The lowest in this range was GZGP, with a Pb^{2+} content of 4.05 mg/kg, and the highest was GZXBX3, with a Pb^{2+} content of 4.50 mg/kg. Four accessions, YNZT, HNHY, JXJA, and ZJLS, had Pb^{2+} content ranging from 5.00 to 6.00 mg/kg. Only GZLL2 had a Pb^{2+} content between 5.00 and 6.00 mg/kg. There were two accessions with Pb^{2+} content ranging from 7.00 to 8.00 mg/kg, which were FJZZ and GZZN. Among the 72 accessions, the one with the highest Pb^{2+} content was GZSCP, with a Pb^{2+} content of 16.77 mg/kg (Table 2).

Table 2: Content of Pb^{2+} in rhizomes of 72 *H. cordata* germplasms

Germplasm	Pb^{2+} Content (mg/kg)	Germplasm	Pb^{2+} Content (mg/kg)	Germplasm	Pb^{2+} Content (mg/kg)
GZZZ	0.32 ± 0.04	GZQT1	2.29 ± 0.28	GZLL3	3.32 ± 0.34
GZNJ1	1.16 ± 0.30	GZXBX2	2.33 ± 0.04	YNDH	3.36 ± 0.55
GZLL7	1.26 ± 0.12	HNXQ	2.33 ± 0.36	CQYY	3.38 ± 0.32
GZXBX1	1.46 ± 0.15	GZNS	2.37 ± 0.24	GZWD	3.48 ± 0.19
GZLZ	1.50 ± 0.07	GZCS3	2.38 ± 0.33	HNYZ	3.68 ± 0.46
GZCS2	1.52 ± 0.08	GZNY	2.39 ± 0.19	HNHH	3.75 ± 0.33
GZLL5	1.55 ± 0.10	HBDY	2.41 ± 0.12	GZLL4	3.76 ± 0.41
GZHX	1.55 ± 0.15	GZNJ2	2.46 ± 0.12	GZQF	3.80 ± 0.13
GZHG	1.61 ± 0.10	GZGSH	2.46 ± 0.11	GZJS	3.95 ± 0.14
GZJA	1.68 ± 0.17	HBZJ	2.52 ± 0.16	SCMS	3.98 ± 0.75
GZLL1	1.75 ± 0.15	GZAS	2.54 ± 0.12	GZGP	4.05 ± 0.27
SCBZ	1.83 ± 0.27	GZQY	2.64 ± 0.05	GZXB2	4.16 ± 0.44
CQXS	1.86 ± 0.24	HNWJP	2.72 ± 0.22	GZLP	4.18 ± 0.10
GZQT2	1.87 ± 0.10	GZTR	2.83 ± 0.24	GZLL6	4.19 ± 0.27
SCNC	1.88 ± 0.25	AHLA	2.83 ± 0.16	YNKM	4.28 ± 0.35
GZXX	1.95 ± 0.13	GZLL8	2.96 ± 0.38	GZXBX3	4.50 ± 0.40
HBTM	1.96 ± 0.08	SCLS	2.97 ± 0.48	YNZT	5.13 ± 0.50
HBES	1.97 ± 0.12	GXLZ	2.98 ± 0.26	HNHY	5.25 ± 0.27
GZBY	1.97 ± 0.29	GZLT	2.98 ± 0.54	JXJA	5.40 ± 0.24
GZLL9	1.99 ± 0.23	CQWX	3.08 ± 0.12	ZJLS	5.78 ± 0.42
GZGY	2.09 ± 0.18	HNCS	3.10 ± 0.35	GZLL2	6.14 ± 0.18
GZPG	2.19 ± 0.09	GZCS1	3.11 ± 0.13	GZZN	7.09 ± 0.22
GZYC	2.20 ± 0.25	GZSD	3.23 ± 0.10	FJZZ	7.98 ± 0.26
GZXB1	2.26 ± 0.16	GZSB	3.27 ± 0.40	GZSCP	16.77 ± 1.50

3.2 RAPD Polymorphic Marker Amplification

Eight RAPD primers were used, resulting in a total of 88 bands, with an average of 11 bands per primer. All 88 bands were polymorphic. The number of bands amplified by each of the primers ranged from 8 to 14. Specifically, the primers produced the following number of bands: OPH-06 amplified 8 bands; OPH-05 amplified 9 bands; OPA-20 amplified 10 bands; OPA-15 and OPH-07 both amplified 11 bands; OPA-10 amplified 12 bands; OPH-19 amplified 13 bands; and the primer with the highest number of bands was OPH-12, which amplified 14 bands (Table 3).

3.3 Correlation Analysis of Pb^{2+} Content and RAPD Markers

Association analysis using a GLM in TASSEL 5.2 revealed seven RAPD loci significantly associated with Pb^{2+} (Fig. 1) content at the nominal level ($p < 0.05$; Table 4), Among them, locus 2 exhibited the highest explanatory power with F = 6.88 and R^2 = 8.94%, followed by locus 33 (R^2 = 7.77%) and locus 43 (R^2 = 6.72%). However, the permutation p-values for all loci exceeded 0.5, indicating that none of the associations remained significant under random phenotype-genotype reshuffling. This suggests that the observed associations may be sensitive to sampling structure, limited sample size, or false positives due to multiple testing.

Table 3: RAPD primer bands statistics

Name of primer	Primer sequences	Maximum number of amplified bands	Number of polymorphic bands	Polymorphism ratio
OPA-10	GTGATCGCAG	12	12	100
OPA-15	TTCCGAACCC	11	11	100
OPA-20	GTTGCGATCC	10	10	100
OPH-05	AGTCGTCCCC	9	9	100
OPH-06	ACGCATCGCA	8	8	100
OPH-07	CTGCATCGTG	11	11	100
OPH-12	ACGCGCATGT	14	14	100
OPH-19	CTGACCAGCC	13	13	100
In total		88	88	
Average		11	11	100

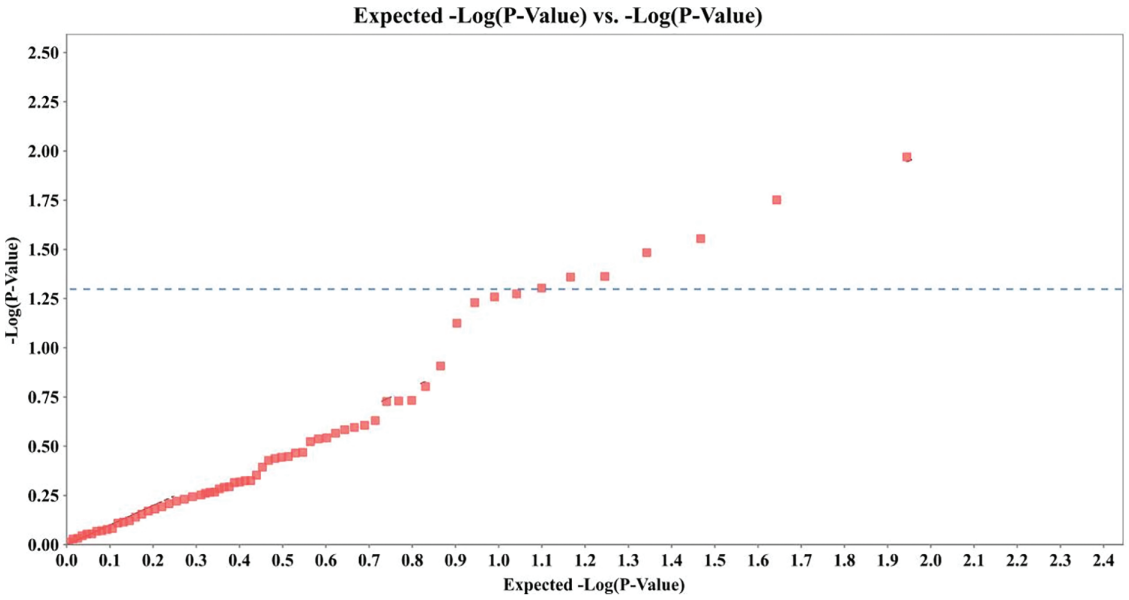

Figure 1: Correlation analysis of Pb^{2+} content and RAPD markers in 72 samples of *H. cordata*. Blue line indicates $p = 0.05$

Table 4: The correlation between RAPD markers and the content of Pb^{2+} in 72 *H.cordata*

RAPD markers	Marker F	Marker *p*	Perm *p*	Marker R^2
Locus 2	6.8753	0.0107	0.5560	8.94%
Locus 33	5.8990	0.0177	0.6760	7.77%
Locus 43	5.0448	0.0279	0.8010	6.72%
Locus 8	4.7401	0.0328	0.8350	6.34%
Locus 27	4.2319	0.0434	0.8990	5.70%

(Continued)

Table 4 (continued)

RAPD markers	Marker F	Marker *p*	Perm *p*	Marker R^2
Locus 30	4.2186	0.0437	0.9020	5.68%
Locus 53	3.9884	0.0497	0.9210	5.39%

Despite this limitation, locus 43 stands out as a candidate marker due to its consistent amplification in high-Pb^{2+}-absorbing accessions (see Table 5), combined with moderate effect size and statistical support ($p = 0.0279$, $R^2 = 6.72\%$). Locus 53, though less significant ($p = 0.0497$), also showed promising group-specific patterns, present in 60% of high absorbers but absent in all low absorbers. These loci are thus prioritized for further validation in larger populations and potential use in marker-assisted selection (MAS).

Table 5: Alidation of Pb^{2+} concentration in *H. cordata* and the existence of Pb^{2+}-related RAPD loci

Germplasm	Pb^{2+} Content (mg/kg)	Locus						
		2	33	43	8	27	30	53
GZZZ	0.32 ± 0.04	0	0	0	1	1	1	0
GZNJ1	1.16 ± 0.30	0	1	0	1	1	1	0
GZLL7	1.26 ± 0.12	1	0	0	1	1	1	0
GZXBX1	1.46 ± 0.15	1	0	0	1	1	0	0
GZLZ	1.50 ± 0.07	1	1	0	1	1	0	0
ZJLS	5.78 ± 0.42	1	1	1	1	1	1	1
GZLL2	6.14 ± 0.18	1	1	1	1	1	1	0
GZZN	7.09 ± 0.22	1	0	1	0	1	1	1
FJZZ	7.98 ± 0.26	0	0	1	1	1	1	1
GZSCP	16.77 ± 1.50	1	0	1	0	0	1	0

The relatively low R^2 values (5.39%–8.94%) across all loci suggest that Pb^{2+} accumulation in *H. cordata* is a polygenic trait, likely controlled by multiple small-effect loci rather than a single dominant gene. Further work involving multi-locus models and genome-wide approaches may help uncover additional genetic factors contributing to lead uptake.

3.4 Verification of the Correlation between Pb^{2+} Content and RAPD Markers

To verify the discriminative power of the seven candidate loci, five accessions with the lowest and five with the highest Pb^{2+} content were selected as an independent panel (Table 5). Locus 43 segregated perfectly between the two groups: it was present in all five high-Pb^{2+} accessions and absent from all five low-Pb^{2+} accessions (sensitivity = 100%, specificity = 100%; two-tailed Fisher's exact $p = 0.008$). This indicates that locus 43 can serve as a diagnostic marker for high Pb^{2+} absorption. Locus 53 was detected in 3/5 high absorbers but in none of the low absorbers (sensitivity = 60%, specificity = 100%; $p = 0.17$), suggesting moderate screening value that needs confirmation in larger populations.Locus 30 showed high sensitivity (100%) but low specificity (40%), while loci 2, 8 and 27 displayed inconsistent patterns and therefore limited predictive value. Collectively, the validation highlights locus 43—and, to a lesser extent, locus 53—as the most reliable

markers for distinguishing Pb^{2+}-high from Pb^{2+}-low germplasms. These loci will be prioritised in subsequent MAS programs aimed at breeding low-Pb^{2+} cultivars of *H. cordata*.

3.5 Patterns of Pb^{2+} Uptake in Different Organs of High/Low Pb^{2+}-Absorbing H. cordata

After validating the relationship between Pb^{2+} absorption and key loci of RAPD molecular markers, we selected two germplasms exhibiting extreme differences in lead absorption capacity-specifically, high and low-to conduct a study on the spatial distribution patterns of endogenous lead in *H. cordata*. After 40 days of post Pb^{2+} treatment, as the concentration of Pb^{2+} increased from 0 to 1000 mg/kg in planting substrate, the Pb^{2+} content in all parts of the two materials, GZNJ1 and GZSCP, increased generally (Table 6). The organ with the highest Pb^{2+} content was the fibrous root, followed by the rhizomes. The Pb^{2+} content in the stem was lower than that in the rhizomes, and the Pb^{2+} content in the leaves was the lowest among the four types of organs. Pb^{2+} content was higher in GZSCP than in GZNJ1 regardless of organ types. The highest Pb^{2+} content was found in the fibrous root of GZSCP at a Pb^{2+} concentration of 1000 mg/kg, which was 29.62 mg/kg, while the lowest content was in the leaves of GZNJ1 at a Pb^{2+} concentration of 0 mg/kg, which was 0.09 mg/kg (Table 6). According to the Chinese National Food Safety Standard (GB 2762-2022), the maximum allowable Pb^{2+} content in vegetables ranges from 0.1 to 0.3 mg/kg (fresh weight), depending on the vegetable type. In this study, the Pb^{2+} concentrations measured in the stems and leaves of the low-absorbing germplasm GZNJ1 under 1000 mg/kg treatment remained relatively low, suggesting a potential for edibility of aerial parts, though further assessment under fresh weight conditions is needed.

Table 6: Pb^{2+} content of *H. cordata* growing parts after 40 d treatments

	Pb^{2+} Tretament (mg/kg)	Fibrous root (mg/kg)	Rhizomes (mg/kg)	Stems (mg/kg)	Leaves (mg/kg)
GZNJ1	0	0.24 ± 0.02 ^{d}	0.12 ± 0.02 ^{d}	0.25 ± 0.03 ^{d}	0.09 ± 0.00 ^{a}
	500	10.18 ± 0.23 ^{c}	3.61 ± 0.06 ^{bc}	1.11 ± 0.06 ^{c}	0.34 ± 0.01 ^{a}
	1000	16.20 ± 0.17 ^{b}	4.15 ± 0.17 ^{b}	1.48 ± 0.09 ^{b}	0.63 ± 0.02 ^{a}
GZSCP	0	0.93 ± 0.14 ^{d}	0.15 ± 0.00 ^{d}	0.31 ± 0.02 ^{d}	0.12 ± 0.01 ^{a}
	500	16.58 ± 0.38 ^{b}	3.10 ± 0.12 ^{c}	1.21 ± 0.02 ^{c}	1.48 ± 1.03 ^{a}
	1000	29.62 ± 0.96 ^{a}	7.90 ± 0.74 ^{a}	1.78 ± 0.10 ^{a}	0.87 ± 0.04 ^{a}

Note: The significant difference markers a–d were compared within the vertical column (the same organ) with $p < 0.05$. a represents the highest mean, b represents a moderately high mean, c represents a moderately low mean, and d represents the lowest mean. There was no significant difference among groups marked with the same letter within the same organ, but there was a significant difference among groups marked with different letters.

3.6 Changes of Membrane Lipid Peroxidation in Different Pb^{2+} Treated H. cordata Organs

In the absence of exogenous Pb^{2+} stress, the MDA content in the fibrous roots was higher than that in the other three organs. The MDA content in the rhizomes was the second highest, followed by that in the stems, and the leaves had the lowest MDA content. Moreover, the MDA level in the low Pb^{2+}-absorbing germplasm (GZNJ1) was higher than that in the high Pb^{2+}-absorbing germplasm (GZSCP), indicating that the biomembrane homeostasis of GZSCP may be higher than that of GZNJ1. When the two *H. cordata* germplasms with high and low Pb^{2+} absorption were subjected to different concentrations of exogenous Pb^{2+} stress, the MDA concentrations in the fibrous roots, rhizomes, stems, and leaves showed an increasing trend with the increase of Pb^{2+} stress intensity. That is, the degree of membrane lipid peroxidation in *H. cordata* is positively correlated with the degree of exogenous Pb^{2+} stress (Fig. 2).

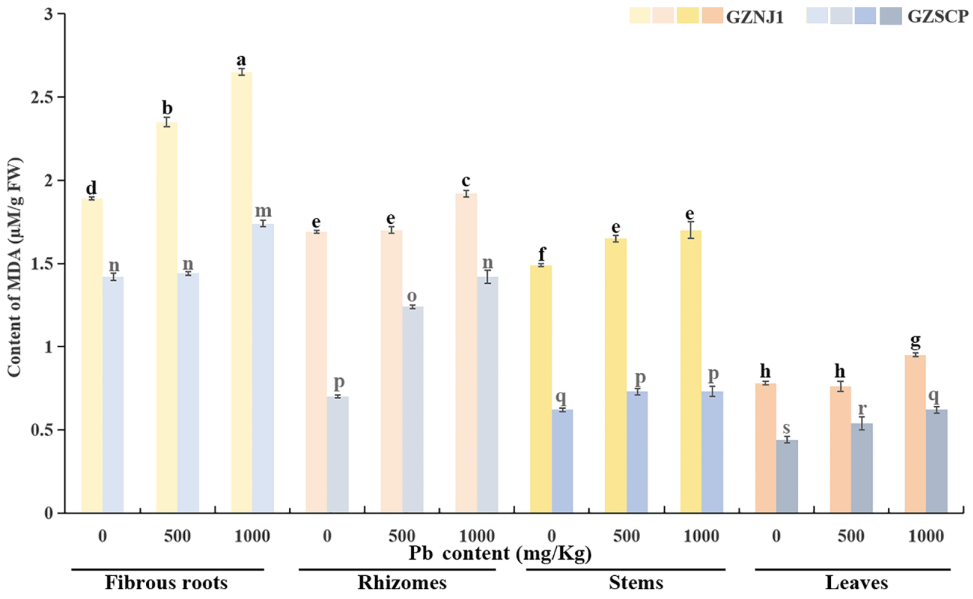

Figure 2: Content of MDA in different Pb^{2+} treated *H. cordata* organs. Data were present by average value ± stand error. The significant differences in data are compared within the same germplasm. The data were analyzed for significant differences at $p < 0.05$

3.7 Changes of Redox Enzyme Activities in Different Pb^{2+} Treated H. cordata Organs

Compared to POD and CAT, the changes in SOD activity across various organs of two *H. cordata* germplasms, exhibited minor variations under exogenous Pb^{2+} stress. Notably, a significant increase in SOD activity was only observed in the fibrous roots of the GZNJ1 germplasm treated with 1000 mg/kg Pb^{2+}, with insignificant changes in SOD activity in organs from other treatments. Similarly, a marked uptrend in SOD activity was evident in the leaves of the GZSCP subjected to 1000 mg/kg Pb^{2+} treatment, whereas minimal alterations were detected in SOD activity among organs from the remaining treatments (Fig. 3).

The POD activity in the various organs of the Pb^{2+}-low-absorbing germplasm (GZNJ1) exhibited a significant upward trend as exogenous Pb^{2+} stress intensified. Among these organs, the POD activity was strongest in the fibrous roots, followed by the rhizomes, then the stems, and finally the leaves, which showed the lowest POD activity. In contrast, within the Pb^{2+}-high-absorbing germplasm (GZSCP), the POD activity was notably altered only in the fibrous roots in response to exogenous Pb^{2+} stress (Fig. 4).

Among the 3 redox enzymes, the CAT activity in various organs of both *H. cordata* germplasms exhibited a significant upward trend with increasing exogenous Pb^{2+} stress, generally. Notably, exposure to 500 and 100 mg/kg of exogenous Pb^{2+} stress significantly induced an enhancement in CAT activity in the fibrous roots and rhizomes. However, in the stems and leaves of the Pb^{2+}-low-absorbing germplasm (GZNJ1), the CAT activity was not markedly induced by exogenous Pb^{2+} stress. Conversely, in the stems and leaves of the Pb^{2+}-high-absorbing germplasm (GZSCP), the CAT activity showed a significant increase in response to exogenous Pb^{2+} stress (Fig. 5).

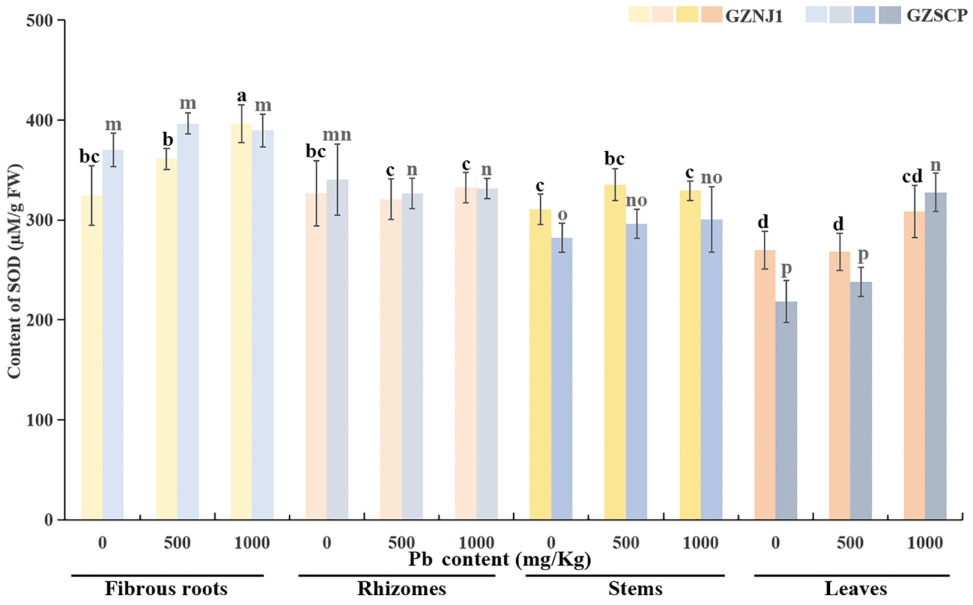

Figure 3: Activities of SOD in different Pb^{2+} treated *H. cordata* organs. Data were present by average value ± stand error. The significant differences in data are compared within the same germplasm. The data were analyzed for significant differences at $p < 0.05$

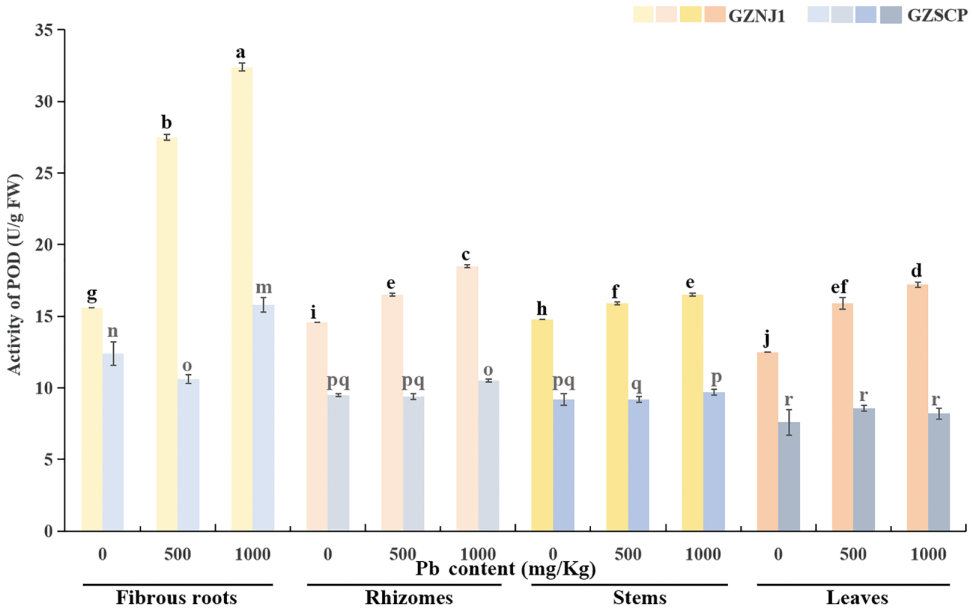

Figure 4: Activities of POD in different Pb^{2+} treated *H. cordata* organs. Data were present by average value ± stand error. The significant differences in data are compared within the same germplasm. The data were analyzed for significant differences at $p < 0.05$

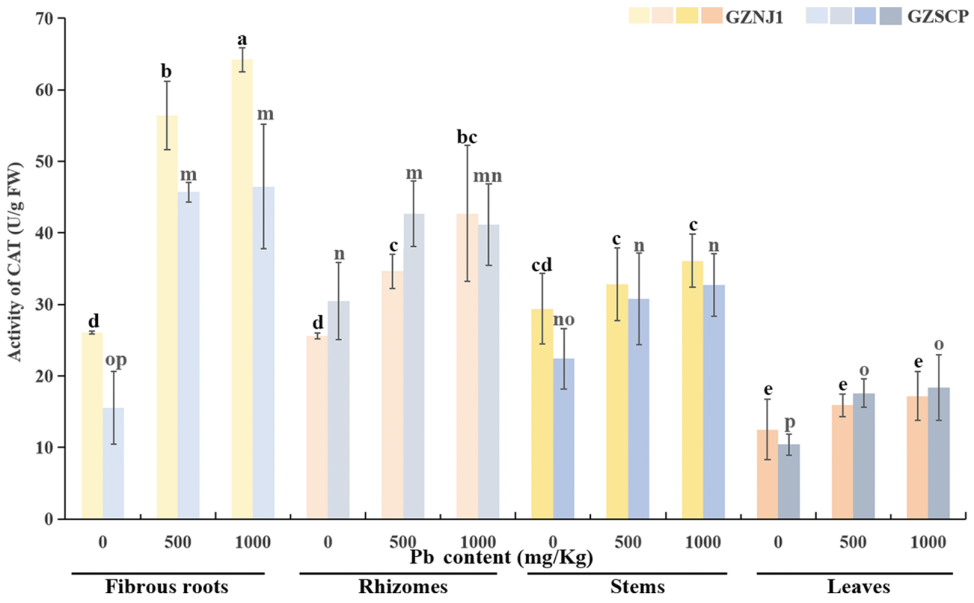

Figure 5: Activities of CAT in different Pb^{2+} treated *H. cordata* organs. Data were present by average value ± stand error. The significant differences in data are compared within the same germplasm. The data were analyzed for significant differences at $p < 0.05$

4 Discussion

The *H. cordata* investigated in this research was primarily collected from southwestern China, where the germplasm exhibited considerable variation in Pb^{2+} absorption capacity, indicating a rich diversity of *H. cordata* germplasm resources in this region. A substantial proportion of the collected *H. cordata* samples exhibited robust Pb^{2+} absorption capabilities, with only a solitary sample recording a concentration below 1 mg/kg (Table 2). The identification of *H. cordata* varieties with low Pb^{2+} absorption holds immense promise for biotechnology-driven breeding programs and the cultivation of low Pb^{2+} absorption varieties. Furthermore, the striking disparities in Pb^{2+} absorption between high and low absorbers offer valuable insights into the molecular mechanisms governing Pb^{2+} absorption in *H. cordata*. By integrating studies on Pb^{2+} absorption in *H. cordata* with RAPD molecular markers, we can pinpoint RAPD loci that are associated with Pb^{2+} absorption. This will enable the efficient screening of *H. cordata* germplasm resources with either high or low Pb^{2+} absorption abilities, thereby furnishing technical support for the molecular-assisted breeding of low Pb^{2+} absorption varieties.

In this study, 500 and 1000 mg/kg Pb^{2+} treatments were chosen to establish a clear physiological response range under pot conditions, based on both preliminary observations and literature on *H. cordata* Pb tolerance. Prior studies have shown that 500–1000 mg/kg often induces marked phenotypic and biochemical changes within short experimental windows, whereas ≥2000 mg/kg typically causes severe growth inhibition or mortality [33–35]. The inclusion of 1000 mg/kg was therefore intended to maximize the detection of genotype- and organ-specific differences—patterns that were indeed most evident at this higher level—while 500 mg/kg served as a moderate stress reference. We acknowledge that these concentrations exceed typical agricultural contamination scenarios (<100 mg/kg in most polluted farmlands), and that direct extrapolation of absolute values from high-dose pot experiments to field conditions must be made with caution. Environmental factors such as soil pH, organic matter content, and nutrient status can markedly affect Pb bioavailability and plant uptake; therefore, follow-up trials under field-relevant Pb levels and varied soil chemistries are planned to test the stability of the marker–phenotype associations reported here.

In our study, loci 43 and 53 were consistently associated with high Pb^{2+} accumulation, suggesting that these RAPD markers may be linked to genes with known roles in heavy-metal tolerance. First, a likely candidate class is ATP-binding cassette (ABC) transporters. Recent work in the hyperaccumulator *Sedum alfredii* identified an ABCC-type transporter (Sa14F190) whose heterologous expression in yeast enhanced vacuolar sequestration and accumulation of Cd^{2+}, thereby reducing cytosolic toxicity [36]. Second, another plausible candidate is phytochelatin synthase (PCS), which catalyzes the synthesis of thiol-rich peptides that chelate heavy metals. For example, heterologous expression of NtPCS1 from *Nicotiana tabacum* increased phytochelatin production and altered Cd^{2+} distribution in host plants, directly impacting metal tolerance [37]. Third, based on these well-documented mechanisms, it is reasonable to hypothesize that loci 43 and 53 in *H. cordata* could tag genomic regions harboring ABC transporter or PCS genes that influence Pb^{2+} uptake and detoxification. We will next validate this linkage by sequencing the RAPD fragments and performing co-segregation analysis in mapping populations, enabling the deployment of these markers in breeding programs for low-Pb cultivars.

RAPD molecular markers require no prior knowledge of DNA sequences, are cost-effective, and offer rapid and effective results [38]. This technology has been successfully applied in the identification of genetic resources of *H. cordata* [32,39]. However, to date, there have been no studies or reports on the use of RAPD molecular markers for identifying the lead adsorption characteristics of *H. cordata*. In this study, a correlation analysis was conducted between the Pb^{2+} absorption capacity and RAPD markers of 72 samples of *H. cordata*. The findings revealed multiple loci associated with Pb^{2+} absorption traits, indicating that Pb^{2+} absorption is not controlled by a single gene but is likely the result of the combined action of multiple genes. Associating Pb^{2+} content with molecular markers facilitates the identification of loci related to Pb^{2+} absorption, providing a theoretical basis for the molecular breeding of *H. cordata* varieties with low Pb^{2+} absorption.

The results of this experiment demonstrate that regardless of the Pb^{2+} absorption property of *H. cordata*, organs with a larger contact area with the cultivation substrate contaminated with Pb^{2+} exhibit stronger Pb^{2+} absorption capacity, leading to higher Pb^{2+} concentrations within those organs. This finding aligns with previous researches. When *Lactuca sativa* was subjected to Pb^{2+} treatment, the Pb^{2+} content in both the roots and stems of the samples increased with the Pb^{2+} content in the cultivation substrate, with the roots containing higher Pb^{2+} levels than the shoots [40]. Studies on the adaptability of three ornamental plants—*Tagetes erecta*, *Solanum nigrum*, and *Mirabilis jalapa*—to Pb^{2+} stress revealed that the growth of their branches and root systems was inhibited to varying degrees under different Pb^{2+} stress conditions, with Pb^{2+} primarily accumulating in the roots [41]. These findings may serve as a preliminary reference for assessing whether the Pb^{2+} content in *H. cordata* grown under polluted conditions approaches or exceeds the permissible lead limits for vegetables established in the Chinese National Food Safety Standard (GB 2762-2022), and may inform future evaluations of its edibility and safety.

Similarly, when 3 varieties of sorghum (*Sorghum bicolor*) were planted in Pb^{2+}-contaminated cultivation substrates with concentrations of 0, 100, 200, 400 and 800 mg/kg, Pb^{2+} was predominantly concentrated in the sorghum roots and increased with the treatment concentration [42]. The consistency between the findings of this study and previous research indicates that Pb^{2+} transport efficiency in plants is relatively low, with metabolism mainly occurring in the underground parts. Strategies such as immobilizing Pb^{2+} in the soil into forms that are not absorbable by plant roots or utilizing molecular biology techniques to study and modify root Pb^{2+} absorption properties could contribute to the development of commercial varieties with reduced Pb^{2+} adsorption. Furthermore, the results of this study indicate that the aerial parts of *H. cordata*, including the stems and leaves, are safer for consumption or medicinal use compared to its edible rhizomes. In situations where consumers cannot purchase commercial varieties with low Pb^{2+} absorption, they should prioritize purchasing products derived from the aerial stems and leaves to ensure safety in use.

As the exogenous Pb^{2+} concentration increased, so did the MDA content in fibrous roots, rhizomes, stems and leaves, indicating an elevated degree of membrane lipid peroxidation in the whole plants of two *H. cordata* germplasms. Notably, this trend was consistent across germplasms exhibiting extreme differences in Pb^{2+} absorption capacity (Fig. 1). This suggests that Pb^{2+} can induce certain oxidative damage in various aerial and subterranean organs. The highest accumulation of MDA was observed in the fibrous roots, followed by the rhizomes, then the stems, with the leaves exhibiting the lowest MDA content (Fig. 2). This distribution pattern mirrors the internal spatial distribution of Pb^{2+} within *H. cordata*, implying a direct correlation between the degree of membrane lipid peroxidation and endogenous Pb^{2+} accumulation (Table 4; Fig. 1). In other words, Pb^{2+} accumulation directly contributes to membrane lipid peroxidation damage in *H. cordata*. Among the germplasms with extreme differences in Pb^{2+} absorption capacity, GZSCP cells demonstrated higher tolerance to Pb^{2+} in their biomembranes, with lower MDA levels compared to GZNJ1, which exhibits lower Pb^{2+} absorption capacity. This could be one of the reasons why GZSCP has a greater capacity to accommodate Pb^{2+} compared to GZNJ1.

The differential responses of redox enzyme activities in various organs of the GZNJ1 and GZSCP to exogenous Pb^{2+} stress provide valuable insights into the mechanisms underlying their Pb^{2+} absorption and tolerance at the level of oxidative stress and reductive remediation. SOD is a primary antioxidant enzyme that catalyzes the dismutation of superoxide radicals into oxygen and hydrogen peroxide, thereby protecting cells from oxidative damage [43]. POD is generally involved in the detoxification of hydrogen peroxide and the reinforcement of cell walls, contributing to plant stress tolerance [44]. CAT is another important antioxidant enzyme that catalyzes the decomposition of hydrogen peroxide into water and oxygen, reducing oxidative stress [45]. SOD can catalyze the conversion of O_2^- into O_2 and H_2O_2, and CAT and POD can further catalyze H_2O_2 into H_2O [46]. In this study, the relatively minor variations in SOD activity across most organs under Pb^{2+} stress suggest that SOD may not serve as the dominant antioxidant mechanism in *H. cordata*'s defense system. However, increases in SOD activity were observed in the fibrous roots of GZNJ1 and the leaves of GZSCP under 1000 mg/kg Pb^{2+} treatment (Fig. 3). This organ and germplasm specific upregulation implies that SOD may play a localized and conditional role in Pb^{2+} stress response—being more active where oxidative damage is most acute or persistent. Together, these findings imply that SOD activity in *H. cordata* is spatially regulated and genetically dependent, which is consistent with the notion that SOD acts as the first line of antioxidant defense, followed by more pronounced downstream detoxification via POD and CAT enzymes [27,43]. This may also be due to the relatively late sampling time in this study, by which SOD may have already completed its initial response phase.

The pronounced increase in fibrous roots of GZNJ1 can be attributed to direct exposure to Pb^{2+}, as root tissues are the primary site of heavy metal uptake and accumulation. Meanwhile, the elevated SOD activity in the leaves of GZSCP suggests a systemic oxidative response, potentially due to long-distance translocation of Pb^{2+} and secondary ROS production in photosynthetically active tissues. The limited SOD activity observed in other tissues may indicate a reliance on downstream H_2O_2 scavenging systems, such as POD and CAT, to complete the detoxification cascade. And our results are consistent with the explanations of Li et al. [47] and Mubeen et al. [48]. The differential responses of SOD, POD, and CAT activities in various organs of the two *H. cordata* germplasms to exogenous Pb^{2+} stress highlight the complexity of plant stress responses. The organ-specific and germplasm-dependent responses suggest that different organs and germplasms have evolved distinct mechanisms to cope with Pb^{2+} stress. Understanding these mechanisms can provide a basis for developing strategies to enhance the tolerance of *H. cordata* to Pb^{2+} pollution, potentially improving its use in phytoremediation efforts [21].

This study investigated the Pb^{2+}-absorption capacity of *H. cordata* germplasm collected from south-western China, revealing considerable variation and thus rich genetic diversity in the region. RAPD analysis

identified seven loci associated with Pb^{2+}-absorption traits, laying a theoretical foundation for MAS. A preliminary "extreme-phenotype" validation—comparing five high- and five low-absorbing accessions—showed that loci 43 and 53 consistently distinguished the two groups, suggesting good diagnostic potential. Nevertheless, broader cross-validation in genetically diverse populations and under multiple environmental conditions is under way to confirm the stability and applicability of these markers.

Our results also showed that organs with larger contact areas with the contaminated substrate (especially fibrous roots) accumulated more Pb^{2+}, whereas aerial parts were comparatively safer for consumption. While the present work centred on Pb^{2+} concentration gradients, we recognise that environmental factors such as soil pH and nutrient availability can markedly influence metal bioavailability, root activity and antioxidant-enzyme expression. To clarify these interactions, we also have launched a follow-up factorial experiment that systematically varies soil pH (5.5, 6.5, 7.5) and macronutrient levels under constant Pb^{2+} exposure. This study will pinpoint the individual and combined contributions of soil chemistry and heavy-metal stress to Pb^{2+} uptake and oxidative responses in *H. cordata*.

The identification of RAPD loci significantly associated with Pb^{2+} accumulation, especially loci 43 and 53, provides a foundation for MAS in breeding *H. cordata*. MAS has been widely employed to accelerate genetic improvements—such as disease resistance or abiotic stress tolerance—by selecting individuals based on linked molecular markers rather than phenotypes [49,50]. In our study, the consistent absence of loci 43 and 53 in low-Pb^{2+} accessions suggests they could act as negative selection markers in MAS pipelines: individuals lacking these bands would be prioritized as candidate low-accumulating germplasms. This strategy would significantly reduce reliance on labor-intensive Pb^{2+} assays and expedite early-generation screening.

Similar RAPD-based MAS approaches have proven effective in developing low heavy-metal accumulating crops. For instance, RAPD markers tightly linked to a cadmium uptake gene were successfully used to screen durum wheat across diverse genotypes [51,52]. In durum wheat, molecular markers such as usw47, Cad-5B and KASP achieved accurate classification of low-Cd accessions (96.2%) from large germplasm pools, significantly improving selection efficiency and reducing phenotyping costs [52].

Based on these precedents, we propose that loci 43 and 53 in *H. cordata* could be incorporated into a two-step MAS framework: first screen seedlings via RAPD-PCR for absence of these markers, then validate Pb^{2+} accumulation in the subset that passes marker screening. Ongoing validation trials across diverse genetic backgrounds and field conditions aim to confirm marker robustness and pave the way for developing Pb^{2+}-safe cultivars.

5 Conclusions

This study reveals the genetic diversity and physiological response mechanisms of lead absorption in *H. cordata*: seven RAPD markers associated with lead absorption were identified, underground organs were found to accumulate significantly higher lead than aerial parts, and antioxidant enzymes (POD, CAT) respond to lead stress by mitigating membrane lipid peroxidation. The findings provide a theoretical basis for molecular breeding of low-lead varieties and environmental remediation applications of high-lead-accumulating germplasms. Furthermore, different germplasms and organs showed varied responses in antioxidant enzyme activities under Pb^{2+} stress, highlighting the complex mechanisms of plant stress responses. These findings offer important insights for developing *H. cordata* varieties with low Pb^{2+} absorption, enhancing their application in phytoremediation, and ensuring consumer safety.

Acknowledgement: Thanks to the Guizhou Highland Specialty Vegetable Green Production Science, Technology Innovation Talent Team (Qiankehe Platform Talent-CXTD [2022] 003), Guizhou Mountain Agriculture Key Core Technology Research Project (GZNYGJHX-2023013), Platform construction project of Engineering Research Center

for Protected Vegetable Crops in Higher Learning Institutions of Guizhou Province (Qian Jiao Ji [2022] No. 040), for their self-help on this project.

Funding Statement: This research is supported by the Guizhou Provincial Department of Agriculture and Rural Affairs, the Guizhou Provincial Department of Science and Technology, and the Guizhou Provincial Department of Education. Funding Project are Guizhou Highland Specialty Vegetable Green Production Science, Technology Innovation Talent Team (Qiankehe Platform Talent-CXTD [2022] 003), Guizhou Mountain Agriculture Key Core Technology Research Project (GZNYGJHX-2023013) and Platform construction project of Engineering Research Center for Protected Vegetable Crops in Higher Learning Institutions of Guizhou Province (Qian Jiao Ji [2022] No. 040).

Author Contributions: Yi Yan: Investigation, Formal analysis, Validation and Writing—original draft; Min He: Methodology and Validation; Feifeng Mao: Methodology and Investigation; Xinyu Zhang: Resources and Supervision; Liyu Wang: Conceptualization, Methodology and Project administration; Jingwei Li: Conceptualization, Funding acquisition, Resources, Writing—review & editing, Resources and Supervision. All authors reviewed the results and approved the final version of the manuscript.

Availability of Data and Materials: All raw data and associated materials are publicly available at Figshare via http://10.6084/m9.figshare.29910008 (accessed on 03 September 2025). This includes Pb accumulation data, RAPD band patterns, physiological measurements, primer sequences, and germplasm accession details.

Ethics Approval: Not applicable.

Conflicts of Interest: The authors declare no conflicts of interest to report regarding the present study.

References

1. Adhikari B, Marasini BP, Rayamajhee B, Bhattarai BR, Lamichhane G, Khadayat K, et al. Potential roles of medicinal plants for the treatment of viral diseases focusing on COVID-19: a review. Phytother Res. 2021;35(3):1298–312. doi:10.1002/ptr.6893.
2. Du H, Ding J, Wang P, Zhang G, Wang D, Ma Q, et al. Anti-respiratory syncytial virus mechanism of *Houttuynia cordata* Thunb exploration based on network pharmacology. Comb Chem High Throughput Screen. 2021;24(8):1137–50. doi:10.2174/1386207324666210303162016.
3. Wu Z, Deng X, Hu Q, Xiao X, Jiang J, Ma X, et al. *Houttuynia cordata* Thunb: an ethnopharmacological review. Front Pharmacol. 2021;12:714694. doi:10.3389/fphar.2021.714694.
4. Rafiq S, Hao H, Ijaz M, Raza A. Pharmacological effects of *Houttuynia cordata* Thunb (*H. cordata*): a comprehensive review. Pharmaceuticals. 2022;15(9):1079. doi:10.1016/j.chemosphere.2020.128243.
5. Wang S, Li L, Chen Y, Liu Q, Zhou S, Li N, et al. *Houttuynia cordata* Thunb. alleviates inflammatory bowel disease by modulating intestinal microenvironment: a research review. Front Immunol. 2023;14:1306375. doi:10.3389/fimmu.2023.1306375.
6. Wei P, Luo Q, Hou Y, Zhao F, Li F, Meng Q. *Houttuynia cordata* Thunb.: a comprehensive review of traditional applications, phytochemistry, pharmacology and safety. Phytomedicine. 2024;123:155195. doi:10.1016/j.phymed.2023.155195.
7. Plaza P, Uhart M, Caselli A, Wiemeyer G, Lambertucci S. A review of lead contamination in South American birds: the need for more research and policy changes. Perspect Ecol Conserv. 2018;16(4):201–7. doi:10.1016/j.pecon.2018.08.001.
8. Vasudevan S, Oturan MA. Electrochemistry: as cause and cure in water pollution-an overview. Environ Chem Lett. 2014;12(1):97–108. doi:10.1007/s10311-013-0434-2.
9. Kushwaha A, Hans N, Kumar S, Rani R. A critical review on speciation, mobilization and toxicity of lead in soil-microbe-plant system and bioremediation strategies. Ecotoxicol Env Saf. 2018;147:1035–45. doi:10.1016/j.ecoenv.2017.09.049.

10. Alsafran M, Usman K, Ahmed B, Rizwan M, Saleem M, Al Jabri H. Understanding the phytoremediation mechanisms of potentially toxic elements: a proteomic overview of recent advances. Front Plant Sci. 2022;13:881242. doi:10.3389/fpls.2022.881242.
11. Fuller R, Landrigan PJ, Balakrishnan K, Bathan G, Bose-O'Reilly S, Brauer M, et al. Pollution and health: a progress update. Lancet Planet Health. 2022;6:e535–47. doi:10.1016/S2542-5196(22)00090-0.
12. Balali-Mood M, Naseri K, Tahergorabi Z, Khazdair MR, Sadeghi M. Toxic mechanisms of five heavy metals: mercury, lead, chromium, cadmium, and arsenic. Front Pharmacol. 2021;12:643972. doi:10.3389/fphar.2021.643972.
13. Bouida L, Rafatullah M, Kerrouche A, Qutob M, Alosaimi AM, Alorfi HS, et al. A review on cadmium and lead contamination: sources, fate, mechanism, health effects and remediation methods. Water. 2022;14(21):3432. doi:10.3390/w14213432.
14. García-Niño WR, Pedraza-Chaverrí J. Protective effect of curcumin against heavy metals induced liver damage. Food Chem Toxicol. 2014;69:182–201. doi:10.1016/j.fct.2014.04.016.
15. Matović V, Buha A, Đukić-Ćosić D, Bulat Z. Insight into the oxidative stress induced by lead and/or cadmium in blood, liver and kidneys. Food Chem Toxicol. 2015;78:130–40. doi:10.1016/j.fct.2015.02.011.
16. Renu K, Chakraborty R, Myakala H, Koti R, Famurewa AC, Madhyastha H, et al. Molecular mechanism of heavy metals (Lead, Chromium, Arsenic, Mercury, Nickel and Cadmium)-induced hepatotoxicity—a review. Chemosphere. 2021;271:129735. doi:10.1016/j.chemosphere.2021.129735.
17. Parida L, Patel TN. Systemic impact of heavy metals and their role in cancer development: a review. Environ Monit Assess. 2023;195(6):766. doi:10.1007/s10661-023-11399-z.
18. Wang Q, Li Z, Feng X, Li X, Wang D, Sun G, et al. Vegetable *Houttuynia cordata* Thunb. as an important human mercury exposure route in Kaiyang county, Guizhou province, SW China. Ecotoxicol Env Saf. 2020;197:110575. doi:10.1016/j.ecoenv.2020.110575.
19. Li Y. Study on the accumulation characteristics of Uranium (U), Cadmium (Cd), Arsenic (As) and Lead (Pb) by hydrophytes *Alisma orientale* and *Houttuynia cordata* [master's thesis]. Mianyang, China: Southwest University of Science and Technology; 2020. (In Chinese). doi:10.27415/d.cnki.gxngc.2020.000841.
20. Zhao M, Yue J, Zhou X, Liang Y. Effects of cadmium and lead stress on antioxidant enzyme system in *Houttuynia cordata* leaves. Sichuan Environ. 2021;40(4):199–204. doi:10.14034/j.cnki.schj.2021.04.027.
21. Liu Z, Cai J, Wang T, Wu L, Chen C, Jiang L, et al. *Houttuynia cordata* hyperaccumulates lead (Pb) and its combination with bacillus subtilis wb600 improves shoot transportation. Int J Agric Biol. 2018;20:621–7. doi:10.17957/IJAB/15.0532.
22. Nie G, Liu A, Ghanizadeh H, Wang Y, Tang M, He J, et al. Natural variation in chromium accumulation and the development of related EST-SSR molecular markers in miscanthus sinensis. Agronomy. 2024;14(7):1458. doi:10.3390/agronomy14071458.
23. Huang Y, Sun C, Min J, Chen Y, Tong C, Bao J. Association mapping of quantitative trait loci for mineral element contents in whole grain rice (*Oryza sativa* L.). J Agric Food Chem. 2015;63(50):10885–92. doi:10.1021/acs.jafc.5b04932.
24. Williams JG, Kubelik AR, Livak KJ, Rafalski JA, Tingey SV. DNA polymorphisms amplified by arbitrary primers are useful as genetic markers. Nucleic Acids Res. 1990;18(22):6531–5. doi:10.1093/nar/18.22.6531.
25. Lynch MMBG, Milligan BG. Analysis of population genetic structure with RAPD markers. Mol Ecol. 1994;3(2):91–9. doi:10.1111/j.1365-294x.1994.tb00109.x.
26. Liu L, Zhang Y, Jiang X, Du B, Wang Q, Ma Y, et al. Uncovering nutritional metabolites and candidate genes involved in flavonoid metabolism in *Houttuynia cordata* through combined metabolomic and transcriptomic analyses. Plant Physiol Biochem. 2023;203:108059. doi:10.1016/j.plaphy.2023.108059.
27. Alhammad BA, Ahmad A, Seleiman MF. Nano-hydroxyapatite and ZnO-NPs mitigate Pb stress in maize. Agronomy. 2023;13(4):1174. doi:10.3390/agronomy13041174.
28. Du L, Yang H, Xie J, Han L, Liu Z, Liu ZM, et al. The potential of *Paulownia fortunei* Hemsl for the phytoremediation of Pb. Forests. 2023;14(6):1245. doi:10.3390/f14061245.
29. Zhao J, Hu H, Gao S, Chen G, Zhang C, Deng W, et al. Pb pollution stress in Alnus cremastogyne monitored by antioxidant enzymes. Forests. 2024;15(7):1100. doi:10.3390/f15071100.

30. Paul V, Sankar MS, Vattikuti S, Dash P, Arslan Z. Pollution assessment and land use land cover influence on trace metal distribution in sediments from five aquatic systems in southern USA. Chemosphere. 2021;263:128243. (In Chinese). doi:10.1016/j.chemosphere.2020.128243.
31. Zhu D, Dong Y, Zhou L, Hua G. Comparison of total RNA isolation methods for folium *Houttuyniae*. J Guangzhou Univ Tradit Chin Med. 2012;29(3):300–4. (In Chinese). doi:10.13359/j.cnki.gzxbtcm.2012.03.026.
32. Wu W, Zheng Y, Chen L, Wei Y, Yan Z, Yang R. RAPD analysis of *Houttuynia cordata* germplasm resources. Acta Pharm Sin. 2002;12:986–92. (In Chinese). doi:10.16438/j.0513-4870.2002.12.018.
33. Li Z. Response of *Houttuynia cordata*. to combined Pb-Zn contamination and its metal accumulation characteristics [master's thesis]. Chengdu, China: Sichuan Agricultural University; 2007. (In Chinese).
34. Li H. Effects of Pb and As stress on the growth and Pb, as enrichment characteristics of *Houttuynia cordata* [master's thesis]. Chengdu, China: Sichuan Agricultural University; 2010. (In Chinese).
35. Zeng Z. Effects of Pb and Cd stress on the physiological characteristics and accumulation effects of *Houttuynia cordata* [master's thesis]. Chengdu, China: Sichuan Agricultural University; 2010.
36. Feng T, He X, Zhuo R, Qiao G, Han X, Qiu W, et al. Identification and functional characterization of ABCC transporters for Cd tolerance and accumulation in *Sedum alfredii* Hance. Sci Rep. 2020;10(1):20928. doi:10.1038/s41598-020-78018-6.
37. Wu C, Zhang J, Chen M, Liu J, Tang Y. Characterization of a *Nicotiana tabacum* phytochelatin synthase 1 and its response to cadmium stress. Front Plant Sci. 2024;15:1418762. doi:10.3389/fpls.2024.1418762.
38. Khabiya R, Choudhary GP, Sairkar P, Silawat N, Jnanesha AC, Kumar A, et al. Unraveling genetic diversity analysis of Indian ginseng (*Withania somnifera* (Linn.) Dunal) insight from RAPD and ISSR markers and implications for crop improvement vital for pharmacological and industrial potential. Ind Crops Prod. 2024;210:118124. doi:10.1016/j.indcrop.2024.118124.
39. Lan Y, Wu L, Qiu B, Gao Y, Shi J. Polymorphisms of RAPD molecular markers in *Houttuynia cordata*. J Zhejiang Univ. 2008;25(3):309–13.
40. Ikkonen E, Kaznina N. Physiological responses of lettuce (*Lactuca sativa* L.) to soil contamination with Pb. Horticulturae. 2022;8(10):951. doi:10.3390/horticulturae8100951.
41. Shao Z, Li M, Zheng J, Zhang J, Lu W. Lead tolerance and enrichment characteristics of three hydroponically grown ornamental plants. Appl Sci. 2023;13(20):11208. doi:10.3390/app132011208.
42. Osman HE, Fadhlallah RS, Alamoudi WM, Eid EM, Abdelhafez AA. Phytoremediation potential of sorghum as a bioenergy crop in Pb-amendment soil. Sustainability. 2023;15(3):2178. doi:10.3390/su15032178.
43. Islam MN, Rauf A, Fahad FI, Emran TB, Mitra S, Olatunde A, et al. Superoxide dismutase: an updated review on its health benefits and industrial applications. Crit Rev Food Sci Nutr. 2022;62(26):7282–300. doi:10.1080/10408398.2021.1913400.
44. Liu X, Lu X, Yang S, Liu Y, Wang W, Wei X, et al. Role of exogenous abscisic acid in freezing tolerance of mangrove *Kandelia obovata* under natural frost condition at near 32° N. BMC Plant Biol. 2022;22(1):593. doi:10.1186/s12870-022-03990-2.
45. Li Y, Zhao X, Jiang X, Chen L, Hong L, Zhuo Y, et al. Effects of dietary supplementation with exogenous catalase on growth performance, oxidative stress, and hepatic apoptosis in weaned piglets challenged with lipopolysaccharide. J Anim Sci. 2020;98(3):skaa067. doi:10.1093/jas/skaa067.
46. Yang F, Zhang H, Wang Y, He G, Wang J, Guo D, et al. The role of antioxidant mechanism in photosynthesis under heavy metals Cd or Zn exposure in tobacco leaves. J Plant Interact. 2021;16(1):354–66. doi:10.1080/17429145.2021.1961886.
47. Li Y, Cheng X, Feng C, Huang X. Interaction of lead and cadmium reduced cadmium toxicity in *Ficus parvifolia* seedlings. Toxics. 2023;11(3):271. doi:10.3390/toxics11030271.
48. Mubeen S, Pan J, Saeed W, Luo D, Rehman M, Hui Z, et al. Exogenous methyl jasmonate enhanced kenaf (*Hibiscus cannabinus*) tolerance against lead (Pb) toxicity by improving antioxidant capacity and osmoregulators. Environ Sci Pollut Res Int. 2024;31(21):30806–18. doi:10.1007/s11356-024-33189-x.
49. Collard BCY, Mackill DJ. Marker-assisted selection: an approach for precision plant breeding in the twenty-first century. Philos Trans R Soc Lond B Biol Sci. 2008;363(1491):557–72. doi:10.1098/rstb.2007.2170.

50. Song L, Wang R, Yang X, Zhang A, Liu D. Molecular markers and their applications in marker-assisted selection (MAS) in Bread Wheat (*Triticum aestivum* L.). Agriculture. 2023;13(3):642. doi:10.3390/agriculture13030642.
51. Penner GA, Bezte LJ, Leisle D, Clarke J. Identification of RAPD markers linked to a gene governing cadmium uptake in durum wheat. Genome. 1995;38(3):543–7. doi:10.1139/g95-070.
52. Alsaleh A, Baloch FS, Sesiz U, Nadeem MA, Hatipoğlu R, Erbakan M, et al. Marker-assisted selection and validation of DNA markers associated with cadmium content in durum wheat germplasm. Crop Pasture Sci. 2022;73(1):66–75. doi:10.1071/CP21317.